Published in final edited form as:
Cancer Biol Ther. 2009 May ; 8(9): 808–819.

Bcl-2 antagonists interact synergistically with bortezomib in DLBCL cells in association with JNK activation and induction of ER stress

Girija Dasmahapatra[1], **Dmitry Lembersky**[1], **Mohamed Rahmani**[1], **Lora Kramer**[1], **Jonathan Friedberg**[4], **Richard I. Fisher**[4], **Paul Dent**[2,3], and **Steven Grant**[1,2,3,*]

[1] Department of Medicine, Massey Cancer Center, Virginia Commonwealth University Health Systems, Richmond, VA USA

[2] Department of Biochemistry, Massey Cancer Center, Virginia Commonwealth University Health Systems, Richmond, VA USA

[3] Institute for Molecular Medicine, Massey Cancer Center, Virginia Commonwealth University Health Systems, Richmond, VA USA

[4] Division of Hematology/Oncology, Department of Medicine and James P. Wilmot Cancer Center, University of Rochester Medical Center, Rochester, NY USA

Abstract

Mechanisms underlying interactions between the proteasome inhibitor bortezomib and small molecule Bcl-2 antagonists were examined in GC- and ABC-type human DLBCL (diffuse lymphocytic B-cell lymphoma) cells. Concomitant or sequential exposure to non- or minimally toxic concentrations of bortezomib or other proteasome inhibitors and either HA14-1 or gossypol resulted in a striking increase in Bax/Bak conformational change/translocation, cytochrome *c* release, caspase activation and synergistic induction of apoptosis in both GC- and ABC-type cells. These events were associated with a sharp increase in activation of the stress kinase JNK and evidence of ER stress induction (e.g., eIF2α phosphorylation, activation of caspases-2 and -4, and Grp78 upregulation). Pharmacologic or genetic (e.g., shRNA knockdown) interruption of JNK signaling attenuated HA14-1/bortezomib lethality and ER stress induction. Genetic disruption of the ER stress pathway (e.g., in cells expressing caspase-4 shRNA or DN-eIF2α) significantly attenuated lethality. The toxicity of this regimen was independent of ROS generation. Finally, HA14-1 significantly increased bortezomib-mediated JNK activation, ER stress induction, and lethality in bortezomib-resistant cells. Collectively these findings indicate that small molecule Bcl-2 antagonists promote bortezomib-mediated mitochondrial injury and lethality in DLBCL cells in association with enhanced JNK activation and ER stress induction. They also raise the possibility that such a strategy may be effective in different DLBCL sub-types (e.g., GC- or ABC), and in bortezomib-resistant disease.

Keywords

bortezomib; proteasome inhibitors; Bcl-2 antagonist; HA14-1; DLBCL; lymphoma

[*]Correspondence to: Steven Grant; Division of Hematology/Oncology; Virginia Commonwealth University/Medical College of Virginia; MCV Station Box 980035; Richmond, VA 23298 USA; Tel.: 804.828.5211; Fax: 804.827.3781; stgrant@vcu.edu.

Note

Supplementary materials can be found at: www.landesbioscience.com/supplement/DasmahapatraCBT8-9-Sup.pdf

Introduction

Diffuse lymphocytic B-cell lymphoma (DLBCL) is the most frequently encountered lymphoma in adults.[1] Although treatment progress, including the development of chemotherapeutic regimens such as R-CHOP or advances in bone marrow transplantation have led to an improved prognosis,[2] many patients become resistant to standard therapy and succumb to their disease. Consequently, novel treatment approaches continue to be sought. Recently, molecular profiling of patients with DLBCL has lead to the identification of three distinct sub-types i.e., germinal center (GC-DLBCL); activated B-cell (ABC-DLBCL), and primary mediastinal (PM-DLBCL), which exhibit distinct differences in signaling pathways, biologic characteristics and responses to therapy.[3,4] Such findings raise the possibility that novel therapies may ultimately be targeted to specific DLBCL sub-types.[4,5]

Bortezomib (Velcade) is a reversible inhibitor of the chymotryptic activity of the 26S proteasome that has been approved for the treatment of multiple myeloma,[6] and more recently for mantle cell lymphoma.[7] However, to date, evidence for the activity of bortezomib in DLBCL has been limited, particularly, in the case of patients with the ABC sub-type, who tend to be resistant to most standard forms of therapy.[2,4,5,8] The mechanisms by which bortezomib or other proteasome inhibitors kill neoplastic cells is not known with certainty, but have been related to sparing of IκBα from proteasomal degradation, leading to sequestration of p65/RelA (NFκB) in the cytoplasm, thereby preventing its nuclear translocation and induction of NFκB-dependent survival genes.[9] Other bortezomib actions linked to lethality in preclinical studies include induction of oxidative damage (e.g., ROS generation)[10] or endoplasmic reticulum stress,[11] and activation of the stress-related pathway JNK (c-Jun N-terminal kinase).[12]

Dysregulation of members of the Bcl-2 family of pro- and anti-apoptotic proteins characteristically occurs in diverse cancers, including lymphoma.[13] Such considerations provided the rationale for the development of small molecules which bind to the BH3 hydrophobic binding groove of the anti-apoptotic proteins Bcl-2 and Bcl-x_L, and in so doing, promote apoptosis. Such agents include HA14-1, gossypol and clinically relevant agents such as ABT-737 and GX15-070 (obatoclax).[14,15] Notably, in preclinical studies, small molecule Bcl-2 antagonists have shown significant activity against lymphoma cells in vitro and in vivo.[16,17]

Previous studies from several laboratories, including our own, have shown that Bcl-2 antagonists potentiate the activity of bortezomib in malignant hematopoietic cells; particularly multiple myeloma cells.[17,18] For example, we have reported that pretreatment of human multiple myeloma cells with bortezomib sensitized them to the lethal effects of HA14-1 through a process involving ROS generation.[18] Very recently, Bcl-2 antagonists have been found to potentiate proteasome inhibitor lethality in mantle cell and other lymphoma cells.[19] Currently, however, the mechanisms by which such interactions occur in DLBCL cells have not been characterized in depth, nor has the efficacy of this strategy been examined in different DLBCL sub-types, (e.g., GC or ABC) or in bortezomib resistant cells. To address these issues, we have examined factors contributing to potentiation of bortezomib lethality by the BH3 peptide-mimetics HA14-1 and gossypol in various DLBCL types. Our results indicate that such agents markedly increase bortezomib-mediated mitochondrial injury and lethality in both ABC and GC DLBCL sub-types. Furthermore, the enhanced lethality of this regimen depends functionally on activation of the stress kinase JNK and induction of endoplasmic reticulum (ER) stress. Finally, similar interactions between HA14-1 and bortezomib also occur in bortezomib-resistant lymphoma cells. Together, these findings provide a mechanistic basis for strategies combining proteasome inhibitors with Bcl-2 antagonists in DLBCL.

Results

HA14-1 interacts synergistically with bortezomib in SUDHL16 cells

Interactions between the proteasome inhibitor bortezomib and HA14-1 were first assessed in SUDHL16 cells, a DLBCL GC subtype Individual exposure (36 hr) to low concentrations of bortezomib (2–4 nM) or HA14-1 (2–3 μM) induced limited lethality (e.g., ~15–24%) cell death. However, combined treatment resulted in a marked increase in cell death e.g., ~65–75% (Fig. 1A), with CI values less than 1.0 by Median Dose effect analysis denoting synergism (Fig. 1A: inset). Notably, pretreatment (8 h) of cells with bortezomib followed by HA14-1 (28 hrs) also led to an increase in cell death (Fig. 1B), although the degree of synergism was slightly less than that observed for simultaneous exposure (Fig. 1B: inset). Such findings contrasted sharply with results of previous studies in multiple myeloma cells in which bortezomib pretreatment was required for optimal interactions with HA14-1.[18] Time course analysis revealed an increase in cell death for HA14-1/bortezomib treatment which was apparent after 12–14 h of exposure, and which increased further over the ensuing 24 h (Fig. 1C). To determine whether similar interactions might occur in primary cells, DLBCL cells obtained from the bone marrow of a DLBCL patient with extensive bone marrow involvement were isolated as above and exposed to 4.0 nM bortezomib ± 3.5 uM HA14-1 for 14 h, after which cell viability was monitored by annexin V/PI staining. As observed in Figure 1D, a pronounced reduction in viability was observed following combined drug treatment, analogous to results obtained in DLBCL lines. Interestingly, identical exposures exhibited minimal toxicity toward normal $CD34^+$ bone marrow progenitor cells (Fig. 1E).

Similar interactions occur in other DLBCL cell types, and with other proteasome inhibitors and Bcl-2 antagonists

Parallel studies were performed in SUDHL4 and SUDHL6 cells (both GC lines), and revealed virtually identical HA14-1/bortezomib interactions as observed with SUDHL16 cells (Suppl. Fig. 1A). A comparable increase in cell death following combined treatment occurred in OCI LY10 lymphoblastic lymphoma cells (ABC-type) (Suppl. Fig. 1B) and as well as OCI LY3 cells (data not shown). In all cases, the time course of cell death closely mimicked that of SUDHL16 cells (data not shown).

To determine whether these findings were restricted to HA14-1 and bortezomib, studies were performed with other proteasome inhibitors (e.g., MG132 and ALLN) or other Bcl-2 antagonists (e.g., gossypol).[25] Combined treatment of SUDHL16 cells with MG132 and HA14-1 resulted in a marked increase in cell death (Suppl. Fig. 1C). Similarly, co-administration of marginally toxic concentrations of ALLN and gossypol resulted in a pronounced increase in lethality in Raji cells (Suppl. Fig. 1C). Together, these findings indicate that interactions between proteasome inhibitors and Bcl-2 antagonists in various DLBCL cell types, including both GC- and ABC sub-types, are not restricted to bortezomib and HA14-1.

Combined exposure of DLBCL cells to bortezomib and HA14-1 induces mitochondrial injury and caspase activation in association with marked JNK activation and evidence of ER stress

Treatment of SUDHL-16 cells for 14 h with minimally toxic concentrations of HA14-1 and bortezomib in combination resulted in a pronounced increase in activation of caspases-3, -9, -7 and -8 as well as release of mitochondrial pro-apoptotic proteins (cytochrome *c* and Smac; Fig. 2A). In accord with these findings, combined, but not individual exposure of cells to these agents induced clear evidence of Bax and Bak conformational change, and diminished association of Bax with Bcl-2 (Fig. 2A). Interestingly, no major changes in

expression levels of Bcl-2 family proteins, including Bcl-2, Bcl-x_L, Mcl-1, NOXA, Bim, PUMA or XIAP were observed, although combined treatment was associated with the appearance of a Bcl-2 cleavage product (Suppl. Fig. 2). Similar results were obtained with other DLBCL lines (e.g., SUDHL6; data not shown).

Effects of the combination were then examined in relation to MAPK signaling in SUDHL16 cells. While individual treatment had little effect, combined treatment resulted in a dramatic increase in phosphorylation of the stress-related JNK kinase and that of its substrate c-Jun (Fig. 2B). On the other hand, minimal changes in ERK phosphorylation were noted. In addition, bortezomib alone induced p38 MAPK phosphorylation, but this was not further enhanced by HA14-1. Thus, combined treatment induced a marked increase in JNK activation in these cells.

In view of evidence linking proteasome inhibitor lethality and induction of ER stress,[11] effects of the combination were examined with respect to several ER stress markers. Whereas individual exposure exerted minimal effects, combined treatment resulted in modest but discernible increases in caspase-2 and caspase-4 cleavage/activation, and phosphorylation of eIF2α,[26] (Fig. 2C). Co-administration of HA14-1 also modestly enhanced bortezomib-mediated induction of the chaperone protein Grp78 and ATF6, an ER membrane-anchored transcription factor and key activator of the unfolded protein response (Fig. 2C). In contrast, the bortezomib/HA14-1 regimen did not discernibly increase expression of IREα, GRP94 (Fig. 2C), or GADD153/CHOP (data not shown) (Fig. 2C).

Time course studies in SUDHL16 cells revealed that combined treatment resulted in the early activation of JNK (i.e., within 2–6 h), whereas ER stress-related events (e.g., eIF2α phosphorylation, caspase-2 and -4 cleavage) were most prominent 10–14 h after drug administration (Fig. 2D).

HA14-1/bortezomib lethality does not primarily involve ROS generation in DLBCL cells

In view of evidence that bortezomib/HA14-1-mediated lethality proceeds through an ROS-dependent process in multiple myeloma cells,[18] the role of ROS in responses of lymphoma cells were then investigated. Exposure (4 h) of SUDHL4 cells to bortezomib (5.0 nM) ± 4.0 μM HA14-1 failed to increase ROS levels appreciably, nor did addition of the antioxidant NAC modify ROS generation (Fig. 3A). In contrast, treatment with the HDAC inhibitor MS-275 (2.0 μM)[27] or H_2O_2 (0.5 mM) resulted in a significant increase in ROS. Significantly, co-administration of L-N-acetylcysteine (NAC failed to protect SUDHL4 cells from bortezomib/HA14-1 lethality (Fig. 3B), nor did it significantly diminish lethality in multiple other DLBCL lines investigated (e.g., SUDHL16, OCI LY10 etc., data not shown). These findings argue against the likelihood that bortezomib/HA14-1 lethality in DLBCL cells stems primarily from ROS generation, in contrast to the results of previous studies involving multiple myeloma cells.[18] In separate studies, expression of GSH, a regulator of ROS generation, did not significantly vary between myeloma and DLBCL cells (data not shown).

Enhanced JNK activation plays a significant functional role in HA14-1/bortezomib lethality and induction of ER stress in DLBCL cells

To gain insights into the functional role of JNK activation in lethality, and its relationship to ER stress induction, both pharmacologic and genetic approaches were employed. Exposure of SUDHL16 cells to bortezomib and HA14-1 in conjunction with the JNK/c-Jun-inhibitory peptide IB1,[28] significantly diminished lethality (Fig. 4A; $p < 0.01$) in association with inhibition of JNK phosphorylation and c-jun phosphorylation (Fig. 4B). Consistent with these findings, shRNA knockdown of JNK significantly diminished bortezomib/HA14-1-

mediated apoptosis (Fig. 4C; $p < 0.02$). Analogously, consistent with results obtained with IB1 (Fig. 4B), shRNA JNK knockdown diminished bortezomib/HA14-1-mediated cleavage of caspases-2 and -4 (Fig. 4D). In separate studies, inhibition of p38 MAPK (i.e., by the inhibitor SB203580) did not diminish bortezomib/HA14-1 lethality or JNK activation (Suppl. Fig. 3A and B). Together, these findings indicate that JNK activation plays a significant functional role in HA14-1/bortezomib lethality.

ER stress induction contributes functionally to bortezomib/HA14-1 lethality in DLBCL cells

To determine whether induction of components of the ER stress pathway induced by bortezomib/HA14-1 treatment contribute functionally to enhanced lethality, OCI LY10 cells stably transfected with either a caspase-4 shRNA or a dominant-negative eIF2α construct. Cells expressing caspase-4 siRNA (Fig. 5A; inset) or DN-eIF2α constructs (Fig. 5B; inset) displayed a partial but significant reduction in lethality compared to scrambled sequence or empty vector controls following bortezomib/HA14-1 exposure ($p < 0.05$ in each case) (Fig. 5A and B). Notably, JNK activation was not attenuated in caspase-4 shRNA cells (Fig. 5C).

HA14-1 potentiates bortezomib lethality in DLBCL and raji cells resistant to bortezomib

To determine whether similar interactions might occur in cells resistant to bortezomib, SUDHL16 and Raji cells that had been adapted to grow in the presence of bortezomib were employed. These cells (e.g., SUDHL16-10BR, Raji-20BR) were maintained in the presence of 10 nM and 20 nM of bortezomib respectively without any impact on cell growth or viability. These cells express equivalent CD20 expression, compared to their parental counterparts, confirming their B-cell origin (Fig. 6A: inset). To rule out the possibility that bortezomib resistance might reflect development of the multi-drug resistance (MDR) phenotype, Pgp expression was monitored by flow cytometry. No increase in Pgp expression was observed in either resistant cell line, nor did cross-resistance to VP-16, a Pgp substrate, occur (data not shown). As shown in Figure 6A, SUDHL16-10BR and Raji-20BR cells displayed minimal toxicity following exposure to bortezomib concentrations of 12 and 25 nM respectively, whereas these concentrations were lethal to essentially 100% of parental cells. However, when SUDHL16-10BR cells were exposed to 12 nM bortezomib in combination with a minimally toxic concentration of HA14-1 (4.0 μM), a prounounced increase in apoptosis (e.g., approximately 75%, Fig. 6A, left) was observed. Very similar findings were obtained in resistant Raji cells exposed to 25 nM bortezomib in conjunction with 5.0 μM HA14-1 (Fig. 6A, right).These findings indicate that co-administration of HA14-1 can enhance bortezomib lethality in cells resistant to bortezomib alone.

HA14-1 promotes bortezomib-mediated JNK activation and ER stress induction in bortezomib-resistant SUDHL16 and raji cells

The effects of HA14-1 on bortezomib-mediated JNK activation and induction of ER stress were then investigated. In parental SUDHL16 cells, bortezomib concentrations as low as 3 nM induced JNK activation, caspase-2 and -4 cleavage, and eIF2α phosphorylation, and effects were very pronounced at slightly higher bortezomib concentrations (e.g., 4–5 nM; Fig. 6B; left). In marked contrast, a bortezomib concentration as high as 12 nM had minimal or no effects on these events in SUDHL16-10BR cells, although some changes were observed with higher bortezomib concentrations (e.g., 15–20 nM) in this line (Fig. 6B, right). Significantly, in SUDHL16-10BR cells, co-administration of 12 nM bortezomib with 5 μM HA14-1, which by itself had little effect, robustly induced JNK phosphorylation, caspase-2 and -4 cleavage, and eIF2α phosphorylation (Fig. 6C). Similar findings were observed in Raji-20BR cells (data not shown). Together, these findings indicate that HA14-1 can lower the threshold for bortezomib-mediated JNK activation, ER stress induction and lethality in DLBCL cells that have developed resistance to bortezomib.

Discussion

Results of the present study provide several novel, insights into the mechanism(s) responsible for synergistic interactions between proteasome inhibitors and small molecule Bcl-2 antagonists in DLBCL cells, and raise the possibility that this strategy may be of therapeutic value in this disorder. In contrast to its established clinical activity in multiple myeloma or mantle cell lymphoma,[6,7] evidence for the activity of bortezomib in DLBCL is limited.[8] Moreover standard therapeutic regimens such as CHOP (with or without Rituximab), are associated with significantly different outcomes in patients with different DLBCL sub-types e.g., GC- vs. ABC. For example, patients with the ABC sub-type tend to have inferior responses to chemotherapy.[2] In this context, the finding that co-administration of bortezomib and Bcl-2 antagonist was equally active against both GC- and ABC type takes on added significance. In addition, several distinct differences were noted in the responses of multiple myeloma cells,[18] another B-cell malignancy, and DLBCL cells, to this strategy. First, in myeloma cells, pretreatment with bortezomib (i.e., for 8 h or more) was required for synergistic interactions with Bcl-2 antagonists,[18] whereas simultaneous drug administration was at least as effective, if not more so, in the case of DLBCL cells. The basis for schedule-dependent differences between the two cell types remains to be determined. In addition, synergistic interactions between bortezomib and Bcl-2 antagonists in multiple myeloma cells were linked functionally to induction of oxidative injury (e.g., ROS generation), reflected by the ability of antioxidants to protect cells from this regimen.[18] Such findings are in accord with evidence that proteasome inhibitors kill transformed cells, at least in part, by inducing ROS.[10] However, in contrast to the results of studies in multiple myeloma cells, combined exposure of DLBCL cells to bortezomib and Bcl-2 antagonist did not generally induce an increase in ROS levels, and lethality was not attenuated by antioxidants. It is possible that in such cells, ROS generation, if it occurs, represents a response to other events (e.g., induction of ER stress)[20] that are primarily responsible for cell death. Together, these findings suggest that despite certain similarities, the mechanisms by which this strategy triggers apoptosis in multiple myeloma and DLBCL exhibit distinct differences.

Recent gene profiling analysis has allowed the sub-typing of DLBCL into distinct subcategories (i.e., GC-DLBCL, ABC-DLBCL and PM-DLBCL) which exhibit clear differences in biologic behavior, signaling characteristics and responses to therapy.[3–5] For example, the ABC-DLBCL sub-type is characterized by increased dependence upon NFκB for survival, and a generally poorer response to therapy than the GC-DLBCL sub-type.[29] It is notworthy that in the present studies, responses of GC-DLBCL cells to regimens combining bortezomib and HA14-1 were very similar if not identical to those of ABC-DLBCL cells. Such findings suggest, albeit indirectly, that the lethality of this strategy involves pathways other than or in addition to those known to distinguish ABC- from GC-related DLBCL. For example, it is possible that mechanisms underlying proteasome/Bcl-2 inhibitor lethality may be independent of effects on NFκB activation. Additional studies will be necessary to confirm or refute this hypothesis.

The bulk of evidence suggests that HA14-1 promotes bortezomib lethality in DLBCL cells by promoting mitochondrial injury, which leads in turn to engagement of the caspase-dependent apoptotic cascade. Mitochondrial injury is induced by activation and/or translocation of the multi-domain pro-apoptotic proteins Bax and Bak, which upon dimerization form channels in the mitochondrial membrane (mitochondrial outer membrane permeabilization; MOMP) allowing egress of pro-apoptotic molecules such as cytochrome *c* and Smac.[30–33] Consistent with this model, combined, but not individual, exposure of DLBCL cells to HA14-1 and bortezomib resulted in a dramatic increase in Bax and Bak conformational change, hallmarks of apoptosis initiation.[34,35] Multi-domain anti-apoptotic proteins such as Bcl-2, Bcl-x_L and Mcl-1 bind to their pro-apoptotic counterparts and

attenuate Bax and Bak activation.[36] It is thought that BH3-mimetics act, at least in part, by binding to anti-apoptotic proteins and antagonizing this association.[37] Previous studies have shown that some Bcl-2 antagonists (e.g., obatoclax) modify the function certain anti-apoptotic proteins (e.g., Mcl-1) and upregulate Bim in multiple myeloma cells.[38] In the present study, no significant changes in the expression of multi-domain anti-apoptotic proteins were observed in DLBCL cells following bortezomib/HA14-1 treatment, nor were changes in levels of BH3-only pro-apoptotic proteins (e.g., Bim, NOXA, PUMA) noted. However, a diminished association of Bcl-2 with Bax was observed in cells treated with both agents, raising the possibility that in this setting, HA14-1 may lower the threshold for bortezomib-mediated Bax, and by extension, Bak activation. An alternative possibility is that as yet to be determined events induced by bortezomib potentiate the ability of HA14-1 to disrupt interactions between Bax and multi-domain anti-apoptotic proteins.

The stress-related MAPK JNK exerts a pro-apoptotic role in cellular responses to diverse noxious stimuli.[39] JNK activation has been implicated in proteasome inhibitor lethality in both hematopoietic[11,22] and non-hematopoietic malignant cells.[40] Induction of apoptosis by JNK activation may proceed through either indirect mechanisms i.e., modulation of the expression of pro- (e.g., Bim)[41] or anti-apoptotic proteins (e.g., Mcl-1),[42] or, alternatively, more directly e.g., by promotion of mitochondrial injury.[43] The failure of the HA14-1/bortezomib regimen to modify expression of pro- and anti-apoptotic proteins in DLBCL cells would argue against the first possibility. The relationship between JNK and components of the ER stress pathway is complex and may be cell context-dependent. For example, in neuronal cells, ER stress induces JNK activation through an ASK1-dependent process,[44] and in fibroblasts by an IREα-dependent mechanism.[45] On the other hand, the JNK-dependent induction of caspase-4 has been implicated in the lethality of bortezomib administered alone in human pancreatic cancer cells.[46] Our findings are most compatible with the latter model. In any case, the finding that pharmacologic or genetic inhibition of JNK significantly attenuated HA14-1/bortezomib lethality argues strongly for a functional role for JNK in the activity of this regimen.

The unfolded protein response (UPR) is an adaptive process by which cells protect themselves from ER-related stresses stemming from accumulation of un- or misfolded proteins.[47] Bortezomib has been shown to induce ER stress in both hematopoietic and non-hematopoietic cells, although its role in the cell death process may be cell-type and context-specific.[48] The findings that genetic interruption of eIF2α phosphorylation and downregulation of caspases-2 and -4, key components of the ER stress response, significantly diminished HA14-1/bortezomib lethality support the notion that ER stress plays a functional role in the toxicity of this regimen in DLBCL cells. Furthermore, the ability of JNK interruption to attenuate these events while protecting cells from apoptosis indicates that at least one component of JNK-mediated lethality in this setting involves induction of ER stress.

It is noteworthy that HA14-1 also potentiated bortezomib lethality in DLBCL cells resistant to bortezomib. Significantly, concentrations of bortezomib that were highly lethal to parental SUDHL or Raji cells were relatively ineffective in triggering JNK activation or ER stress in their resistant counterparts. Such findings are consistent with previous reports demonstrating important functional roles for JNK activation and ER stress induction in proteasome inhibitor lethality in cells sensitive to such agents.[10–12] Notably, co-administration of HA14-1 lowered the threshold for bortezomib-mediated activation of JNK and induction of ER stress as well as lethality in resistant cells. However, it may be significant that interactions between these agents in resistant cells occurred at bortezomib concentrations higher than those required in parental cells, suggesting that HA14-1 cannot completely reverse bortezomib resistance.

In summary, the present studies indicate that small molecule Bcl-2 antagonists synergistically potentiate bortezomib activity in diverse DLBCL types through a process that involves potentiation of mitochondrial injury, activation of the stress-related kinase JNK, and induction of ER stress. They also suggest that in contrast to the case of multiple myeloma cells, in which pretreatment with bortezomib was required for potentiation of Bcl-2 antagonist lethality,[18] interactions in DLBCL cells are schedule independent and do not primarily involve oxidative injury/ROS generation. Such findings could have implications for the rational design of regimens targeting patients with DLBCL. Significantly, the present findings also indicate that Bcl-2 antagonists can enhance bortezomib lethality in DLBCL cells that display resistance to bortezomib alone. The ultimate effectiveness of this strategy in DLBCL will depend upon multiple factors, including the ability of regimens to induce cell death in lymphoma cells selectively. In view of evidence that proteasome inhibitors[49] and Bcl-2 antagonists preferentially kill transformed cells,[50] the finding that the bortezomib/HA14-1 regimen displayed minimal toxicity toward normal hematopoietic cells, as well as recent reports of the in vivo activity of such regimens,[19] further attempts to explore this therapeutic strategy appear warranted. Lastly, the present results raise the possibility that JNK activation or evidence of ER stress induction in tumor tissues may represent plausible laboratory correlates to monitor in conjunction with future clinical trials in which proteasome inhibitors are combined with small molecule Bcl-2 antagonists in patients with DLBCL. Validation of these events as molecular response determinants could also be of use in attempts to optimize drug selection and scheduling in future clinical studies.

Materials and Methods

Cells

Raji human Burkitt's leukemia cells were purchased from American Type Culture Collection, Manassas, VA. SUDHL16 cells (GC subtype) was a kind gift from Dr. Alan Epstein, University of Southern California, LA. SUDHL4, SUDHL6 (both GC), OCI-LY10, OCI-LY3 (both ABC) were provided by Dr. Lisa Rimsza of University of Arizona, Tucson. Bortezomib-resistant SUDHL-10BR (GC) and Raji-20BR were generated by exposing the respective parental cells to progressively increasing concentrations of bortezomib beginning with 1.0 nM. Once cells developed resistance to bortezomib, they were cultured in the absence of drug for 2 w prior to experiments. Multiple studies documented the persistence of drug resistance under these conditions. SUDHL16-sh-JNK cells were generated by electroporation (Amaxa, GmbH, Germany) using buffer L of a MAP8 shRNA (SuperArray Bioscience Corporation, Frederick, MD) into SUDHL16 parental cells according to the manufacturer's instructions. Stable clones were selected by serial dilution using G418 as selection marker. For SUDHL16 cells stably expressing shRNA directed against caspase-4, cDNA oligonucleotides containing the targeted sequence were synthesized, annealed and cloned into the pSUPER.retro-neo vector (Oligoengine, Seattle, WA) using standard techniques. The sequences used for caspase-4 was 5′-ATG TAC TGA ACT GGA AGG AA-3′.[20] Human dominant-negative eIF2α (eIF2α-DN) cDNA was PCR amplified from pCMV-eIF2-S51A and cloned into pcDNA3.1/V5-His (Invitrogen) in frame with the V5 peptide. Stable clones expressing eIF2α-DN were generated using standard techniques described above.[20]

Reagents

Bortezomib (Velcade) was provided by Millennium Pharmaceuticals, Cambridge, MA. HA14-1 and gossypol were purchased from Biomol (Plymouth Meeting, PA, and USA). JNK inhibitor (ALX-159-600) was obtained from Axxora Platform, San Diego, CA. MS-275 was supplied by CTEP/NCI.

Experimental format

Logarithmically growing cells were suspended in sterile plastic T-flasks (Corning, NY) to which the designated drugs were added. The flasks were then placed in a 5% CO_2, 37°C incubator for various intervals. At the end of the incubation period, cells were transferred to sterile centrifuge tubes, pelleted by centrifugation at 400 xg for 10 min at room temperature, and prepared for analysis as described below. All experiments were performed using passages 6–24 of the respective cell lines and equivalent cell concentrations (e.g., 4.0×10^5 cells/ml) were utilized to ensure conformity of drug responses.

Assessment of cell death

Drug effects on cell viability were monitored by flow cytometry using 7AAD as the staining dye as previously described.[21] Briefly, cells were stained with 25 μM 7AAD solution at room temperature in regular culture media and analyzed in the FL2 channel using the Becton Dickinson flow cytometer. Alternatively, cells were washed with 1x PBS and stained with Annexin V/PI (BD PharMingen, San Diego, CA) for 30 min at room temperature. Cells were then processed and analyzed using the cytofluorometer. Cells were also analyzed for viability using the VIACOUNT reagent in conjunction with a GUAVA PCA instrument using CytoSoft software as per the manufacturer's instructions. Results were also verified by Trypan blue staining and enumeration of Trypan blue excluding cells using a hemocytometer. Results for each of these methods were found to be in good agreement.

Assessment of apoptosis

Following drug exposure, cells were stained with Annexin V/PI as described previously.[22] Briefly, cells were washed with 1x PBS and stained with Annexin V/PI (BD PharMingen, San Diego, CA) for 30 min at room temperature. Cells were then processed and analyzed using a Becton-Dickinson FACScan cytofluorometer (Mansfield, MA) in conjunction with Cell Quest software. Cells were considered to be apoptotic if they were either annexin V^+/PI^- (early apoptotic) or annexin V^+/PI^+ (late apoptotic).

Preparation of S-100 fractions and assessment of cytochrome *c* and Smac release

Cells (4×10^6) were lysed by incubating for 1 min in 100 μl of lysis buffer containing 75 mM NaCl, 8 mM Na_2HPO4, 1 mM NaH_2PO_4, 1 mM EDTA, 250 mM Sucrose and 350 μg/ml digitonin. The lysates were centrifuged at 12,000 xg for 1 min and the supernatant was considered as the S-100 cytosolic fraction.

Collection and processing of primary normal $CD34^+$ and DLBCL cells

Normal human bone marrow mononuclear cells were obtained with informed consent from the bone marrow of patients undergoing routine bone marrow aspirations for non-myeloid hematologic disorders. These studies have been approved by the Investigational Review Board of Virginia Commonwealth University. Bone marrow samples were collected in sterile syringes containing heparin and processed by standard techniques to separate mononuclear cells, after which $CD34^+$ cells were isolated using an immunomagnetic bead separation technique as we have previously described in detail.[22] $CD34^+$ cells were then suspended in RPMI1640 medium containing 10% FCS and exposed to agents as described above for continuously cultured cell lines.

Parallel studies were performed on primary DLBCL cells obtained from the bone marrow of a patient with DLBCL and extensive marrow infiltration (>70%). Mononuclear cells were isolated as described above and exposed to HA14-1 ± bortezomib in an identical matter.

Western blot analysis

Western blot samples were prepared from whole cell pellets. Equal amounts of protein (30 μg) were separated by 4–12% Bis-Tris (Invitrogen) precast gel and probed with primary antibodies of interest as we have described in detail previously.[22] The sources of primary antibodies were as follows: AIF, cytochrome *c*, p-JNK, JNK1, p-ERK, ERK, Mcl-1, Bak, Bid, Bcl-$x_{L,}$ CD20, Bax, Bak, IREα, GRP94, GRP78, XBP, p-c-Jun, c-Jun, NOXA, Bim and PUMA were from Santa Cruz Biotechnology, Santa Cruz, CA; cleaved caspase-8, cleaved caspase-3, p-p38, p38, p-eIF2a, eIF2a, CF Caspase 9 were from Cell Signaling Technology, Beverly, MA; Caspase-7, Caspase-2, Mcl-1, XIAP were from BD prarmingen (Transduction Laboratories), Lexington, KY; PARP (C-2-10), Smac was from Upstate Biotechnology, Lake Placid, NY; Caspase-8 was from Alexis, San Diego, CA; Tubulin was from Oncogene, San Diego, CA. Actin was purchased from Sigma, MO. Bcl-2 was from Dako, CA. Caspase-4 was obtained from Stressgene Bioreagents, Ann, MI. Secondary antibodies were obtained from KPL Protein Research Products, Gaithersburg, MD, USA.

Measurement of ROS generation

Cells were exposed to agents for desired time interval, after which they were treated with 2 uM 5-(and-6)-chloromethyl-2′,7′-dichlorodihydrofluorescein diacetate, acetyl ester (molecular probes) for 30 min at 37°C. Fluorescence was then monitored by flow cytometry using a fluorescence-activated cell sorter, and the percentage of cells exhibiting increased ROS levels, reflected by a rightward shift in the curve, determined using Cell Quest software (Becton Dickinson, Palo Alto, CA) as previously described in detail.[22]

TUNEL assay

Slide preparations were made using 100 ml aliquots of each sample which were applied to the slides by cytospin. TUNEL assays were then performed as per standard protocols. In brief, cells were fixed in 4% formaldehyde/PBS for 10 min at room temperature in coplin jar followed by two times washings with PBS. Cells were then permeabilized by treating with 1:2 acetic acid/ethanol solutions for 5 min at RT. Slides were rinsed twice with PBS to remove the acid residue. Cells were then blocked with 1 mg/ml BSA solution prepared in PBS for one hour in RT inside dark humidified chamber and subsequently cells were washed twice with PBS. Slides were stained with fluorescein-12-dUTP using a terminal transferase recombinant kit (Roche, Indianapolis, IN, cat no 1373 242 & 220582 kit) as per the manufacturer's protocol. Slides were then rinsed twice with PBS and stained with vectashield and propidium iodide (PI) (vectashield, Burlingame, CA, cat no H-1200). Finally, slides were mounted with cover slips, dried and sealed with nail polish. Slides were visualized using a fluorescence microscope to identify TUNEL-positive cells and photomicrographs obtained using an Olympus BX40 microscope.

Isolation of mitochondrial fractions

Mitochondrial cell fractions were isolated using a mitochondria isolation kit obtained from Pierce as per the manufacturer's instruction. Cells (2×10^7) were pelleted by centrifugation at 850 *g* for 2 min and were resuspended in 800 μl of reagent A in microcentrifuge tubes. Cells were then incubated in ice for 2 min and subsequently homogenized in a pre-cooled Dounce tissue grinder applying 40–50 strokes. Reagent C (800 μl) was added to the homogenized solution and thoroughly mixed by repeated inversion. The solution was then centrifuged at 700 *g* for 10 min, and the pellet discarded. The supernatant was further centrifuged at 12,000 *g* for 15 min, and the pellet, reflecting intact mitochondria, was further lysed in lysis buffer[23] and subjected to western blot analysis.

Bax and BAK translocation and conformational change

Mitochondrial-rich cell fractions were prepared as described above, washed with Ca^{2+}/Mg^{2+}-free PBS, and lysed with the CHAPS lysis buffer (10 mM HEPES, pH 7.4, 150 mM NaCl, 1% CHAPS and 1 mM DTT) supplemented with protease and phosphatase inhibitors. Two milligrams of anti-Bax (6A7) monoclonal antibody or BAK antibody were preincubated with 30 μl of Dynabeads (M-450), (Dynal Biotech Inc., Lake Success, NY) for 2 h at 4°C. A total of 500 to 1,000 μg of protein was then added to the anti-Bax or BAK antibody loaded with Dynabeads and maintained on a rotor overnight at 4°C. Dynabeads were collected using a Dynal Biotech magnetic particle concentrator and washed four times with CHAPS lysis buffer. Conformationally changed Bax or BAK protein was eluted from the Dynabeads by heating with 4x protein gel loading buffer (Invitrogen) and subjected to western blotting.[23]

Statistical analysis

The significance of differences between experimental conditions was determined using the two-tailed Student's t-test. Assessment of synergistic or antagonistic interactions as well as fractional effects (FA) were determined using Median Dose Effect analysis in conjunction with a commercially available software program (CalcuSyn, Biosoft, Ferguson, MO).[24] In brief cells were treated with bortezomib or HA14-1 either alone or in combination at a fixed concentration ratio (bortezomib: HA14-1::1:1,000). The percentage of apoptotic cells relative to controls (i.e., the fractional effect) in treated samples was determined, and the degree of synergy was assessed by calculating the combination index (CI) values which reflect the degree of synergism or antagonism according to the algorithms described by Chou and Talaly[24] CI values <1.0 correspond to synergistic interactions.

Supplementary Material

Refer to Web version on PubMed Central for supplementary material.

Acknowledgments

These studies were supported by awards CA63753, CA93738 and CA100866 from the National Institutes of Health; award R6059-06 from the Leukemia and Lymphoma Society of America, the Multiple Myeloma Research Foundation, the V Foundation and Lymphoma SPORE award 1P50 CA130805.

Abbreviation

DLBCL	diffuse lymphocytic B-cell lymphoma
GC	germinal center
ABC	activated B-cell

References

1. Coiffier, B. Non-Hodgkin's lymphomas. In: Cavalli, F.; Hansen, HH.; Kaye, SB., editors. Textbook of medical oncology. London: Martin Dunitz; 1997. p. 34-5.
2. Coiffier B, Lepage E, Briere J, Herbrecht R, Tilly H, Bouabdallah R, et al. CHOP chemotherapy plus rituximab compared with CHOP alone in elderly patients with diffuse large-B-cell lymphoma. N Engl J Med 2002;346:235–42. [PubMed: 11807147]
3. Alizadeh AA, Eisen MB, Davis RE, Ma C, Lossos IS, Rosenwald A, et al. Distinct types of diffuse large B-cell lymphoma identified by gene expression profiling. Nature 2000;403:503–11. [PubMed: 10676951]

4. Rosenwald A, Wright G, Chan WC, Connors JM, Campo E, Fisher RI, et al. The use of molecular profiling to predict survival after chemotherapy for diffuse large-B-cell lymphoma. N Engl J Med 2002;346:1937–47. [PubMed: 12075054]
5. Lossos IS, Jones CD, Warnke R, Natkunam Y, Kaizer H, Zehnder JL, et al. Expression of a single gene, BCL-6, strongly predicts survival in patients with diffuse large B-cell lymphoma. Blood 2001;98:945–51. [PubMed: 11493437]
6. Richardson PG, Barlogie B, Berenson J, Singhal S, Jagannath S, Irwin D, et al. A phase 2 study of bortezomib in relapsed, refractory myeloma. N Engl J Med 2003;348:2609–17. [PubMed: 12826635]
7. Fisher RI, Bernstein SH, Kahl BS, Djulbegovic B, Robertson MJ, de Vos S, et al. Multicenter phase II study of bortezomib in patients with relapsed or refractory mantle cell lymphoma. J Clin Oncol 2006;24:4867–74. [PubMed: 17001068]
8. Goy A, Younes A, McLaughlin P, Pro B, Romaguera JE, Hagemeister F, et al. Phase II study of proteasome inhibitor bortezomib in relapsed or refractory B-cell non-Hodgkin's lymphoma. J Clin Oncol 2005;23:667–75. [PubMed: 15613697]
9. Jeong SJ, Pise-Masison CA, Radonovich MF, Park HU, Brady JN. A novel NFkappaB pathway involving IKKbeta and p65/RelA Ser-536 phosphorylation results in p53 Inhibition in the absence of NFkappaB transcriptional activity. J Biol Chem 2005;280:10326–32. [PubMed: 15611068]
10. Ling YH, Liebes L, Zou Y, Perez-Soler R. Reactive oxygen species generation and mitochondrial dysfunction in the apoptotic response to Bortezomib, a novel proteasome inhibitor, in human H460 non-small cell lung cancer cells. J Biol Chem 2003;278:33714–23. [PubMed: 12821677]
11. Fribley A, Zeng Q, Wang CY. Proteasome inhibitor PS-341 induces apoptosis through induction of endoplasmic reticulum stress-reactive oxygen species in head and neck squamous cell carcinoma cells. Mol Cell Biol 2004;24:9695–704. [PubMed: 15509775]
12. Catley L, Tai YT, Shringarpure R, Burger R, Son MT, Podar K, et al. Proteasomal degradation of topoisomerase I is preceded by c-Jun NH2-terminal kinase activation, Fas upregulation and poly(ADP-ribose) polymerase cleavage in SN38-mediated cytotoxicity against multiple myeloma. Cancer Res 2004;64:8746–53. [PubMed: 15574786]
13. Certo M, Del Gaizo Moore V, Nishino M, Wei G, Korsmeyer S, Armstrong SA, et al. Mitochondria primed by death signals determine cellular addiction to antiapoptotic BCL-2 family members. Cancer Cell 2006;9:351–65. [PubMed: 16697956]
14. Tse C, Shoemaker AR, Adickes J, Anderson MG, Chen J, Jin S, et al. ABT-263: a potent and orally bio-available Bcl-2 family inhibitor. Cancer Res 2008;68:3421–8. [PubMed: 18451170]
15. Konopleva M, Watt J, Contractor R, Tsao T, Harris D, Estrov Z, et al. Mechanisms of antileukemic activity of the novel Bcl-2 homology domain-3 mimetic GX15-070 (obatoclax). Cancer Res 2008;68:3413–20. [PubMed: 18451169]
16. Vogler M, Dinsdale D, Sun XM, Young KW, Butterworth M, Nicotera P, et al. A novel paradigm for rapid ABT-737-induced apoptosis involving outer mitochondrial membrane rupture in primary leukemia and lymphoma cells. Cell Death Differ 2008;15:820–30. [PubMed: 18309326]
17. Pérez-Galán P, Roué G, Villamor N, Campo E, Colomer D. The BH3-mimetic GX15-070 synergizes with bortezomib in mantle cell lymphoma by enhancing Noxa-mediated activation of Bak. Blood 2007;109:4441–9. [PubMed: 17227835]
18. Pei XY, Dai Y, Grant S. The proteasome inhibitor bortezomib promotes mitochondrial injury and apoptosis induced by the small molecule Bcl-2 inhibitor HA14-1 in multiple myeloma cells. Leukemia 2003;17:2036–45. [PubMed: 14513055]
19. Paoluzzi L, Gonen M, Bhagat G, Furman RR, Gardner JR, Scotto L, et al. The BH3-only mimetic ABT-737 synergizes the anti-neoplastic activity of proteasome inhibitors in lymphoid malignancies. Blood 2008;112:2906–16. [PubMed: 18591385]
20. Rahmani M, Davis EM, Crabtree TR, Habibi JR, Nguyen TK, Dent P, et al. The kinase inhibitor sorafenib induces cell death through a process involving induction of endoplasmic reticulum stress. Mol Cell Biol 2007;27:5499–513. [PubMed: 17548474]
21. Philpott NJ, Turner AJ, Scopes J, Westby M, Marsh JC, Gordon-Smith EC, et al. The use of 7-amino actinomycin D in identifying apoptosis: simplicity of use and broad spectrum of application compared with other techniques. Blood 1996;87:2244–51. [PubMed: 8630384]

22. Dasmahapatra G, Rahmani M, Dent P, Grant S. The tyrphostin adaphostin interacts synergistically with proteasome inhibitors to induce apoptosis in human leukemia cells through a reactive oxygen species (ROS)-dependent mechanism. Blood 2006;107:232–40. [PubMed: 16166589]
23. Dasmahapatra G, Almenara JA, Grant S. Flavopiridol and histone deacetylase inhibitors promote mitochondrial injury and cell death in human leukemia cells that overexpress Bcl-2. Mol Pharmacol 2006;69:288–98. [PubMed: 16219908]
24. Chou TC, Talalay P. Quantitative analysis of dose-effect relationships: the combined effects of multiple drugs or enzyme inhibitors. Adv Enzyme Regul 1984;22:27–55. [PubMed: 6382953]
25. Meng Y, Tang W, Dai Y, Wu X, Liu M, Ji Q, et al. Natural BH3 mimetic (−)-gossypol inhibition accompanied by increase of chemosensitizes human prostate cancer via Bcl-x_L Puma and Noxa. Mol Cancer Ther 2008;7:2192–202. [PubMed: 18645028]
26. Yan W, Frank CL, Korth MJ, Sopher BL, Novoa I, Ron D, et al. Control of PERK eIF2alpha kinase activity by the endoplasmic reticulum stress-induced molecular chaperone P58IPK. Proc Natl Acad Sci USA 2002;99:15920–5. [PubMed: 12446838]
27. Rosato RR, Almenara JA, Grant S. The histone deacetylase inhibitor MS-275 promotes differentiation or apoptosis in human leukemia cells through a process regulated by generation of reactive oxygen species and induction of p21CIP1/WAF1 1. Cancer Res 2003;63:3637–45. [PubMed: 12839953]
28. Borsello T, Clarke PG, Hirt L, Vercelli A, Repici M, Schorderet DF, et al. A peptide inhibitor of c-Jun N-terminal kinase protects against excitotoxicity and cerebral ischemia. Nat Med 2003;9:1180–6. [PubMed: 12937412]
29. Lam LT, Davis RE, Pierce J, Hepperle M, Xu Y, Hottelet M, et al. Small molecule inhibitors of IkappaB kinase are selectively toxic for subgroups of diffuse large B-cell lymphoma defined by gene expression profiling. Clin Cancer Res 2005;11:28–40. [PubMed: 15671525]
30. Wang X. The expanding role of mitochondria in apoptosis. Genes Dev 2001;15:2922–33. [PubMed: 11711427]
31. Du C, Fang M, Li Y, Li L, Wang X. Smac, a mitochondrial protein that promotes cytochrome *c*-dependent caspase activation by eliminating IAP inhibition. Cell 2000;102:33–42. [PubMed: 10929711]
32. Verhagen AM, Ekert PG, Pakusch M, Silke J, Connolly LM, Reid GE, et al. Identification of DIABLO, a mammalian protein that promotes apoptosis by binding to and antagonizing IAP proteins. Cell 2000;102:45–53.
33. Susin SA, Lorenzo HK, Zamzami N, Marzo I, Snow BE, Brothers GM, et al. Molecular characterization of mitochondrial apoptosis-inducing factor. Nature 1999;397:441–6. [PubMed: 9989411]
34. Zha H, Aime-Sempe C, Sato T, Reed JC. Proapoptotic protein Bax heterodimerizes with Bcl-2 and homodimerizes with Bax via a novel domain (BH3) distinct from BH1 and BH2. J Biol Chem 1996;271:7440–4. [PubMed: 8631771]
35. Mohan J, Gandhi AA, Bhavya BC, Rashmi R, Karunagaran D, Indu R, et al. Caspase-2 triggers Bax-Bak-dependent and -independent cell death in colon cancer cells treated with resveratrol. J Biol Chem 2006;281:17599–611. [PubMed: 16617056]
36. Willis SN, Chen L, Dewson G, Wei A, Naik E, Fletcher JI, et al. Proapoptotic Bak is sequestered by Mcl-1 and Bcl-x_L, but not Bcl-2, until displaced by BH3-only proteins. Genes Dev 2005;19:1294–305. [PubMed: 15901672]
37. Labi V, Grespi F, Baumgartner F, Villunger A. Targeting the Bcl-2-regulated apoptosis pathway by BH3 mimetics: a breakthrough in anticancer therapy? Cell Death Differ 2008;15:977–87. [PubMed: 18369371]
38. Trudel S, Li ZH, Rauw J, Tiedemann RE, Wen XY, Stewart AK. Preclinical studies of the pan-Bcl inhibitor obatoclax (GX015-070) in multiple myeloma. Blood 2007;109:5430–8. [PubMed: 17332241]
39. Tournier C, Hess P, Yang DD, Xu J, Turner TK, Nimnual A, et al. Requirement of JNK for stress-induced activation of the cytochrome *c*-mediated death pathway. Science 2000;288:870–4. [PubMed: 10797012]

40. Yang Y, Ikezoe T, Saito T, Kobayashi M, Koeffler HP, Taguchi H. Proteasome inhibitor PS-341 induces growth arrest and apoptosis of non-small cell lung cancer cells via the JNK/c-Jun/AP-1 signaling. Cancer Sci 2004;95:176–80. [PubMed: 14965369]
41. Biswas SC, Shi Y, Sproul A, Greene LA. Pro-apoptotic Bim induction in response to nerve growth factor deprivation requires simultaneous activation of three different death signaling pathways. J Biol Chem 2007;282:29368–74. [PubMed: 17702754]
42. Inoshita S, Takeda K, Hatai T, Terada Y, Sano M, Hata J, et al. Phosphorylation and inactivation of myeloid cell leukemia 1 by JNK in response to oxidative stress. J Biol Chem 2002;277:43730–4. [PubMed: 12223490]
43. Aoki H, Kang PM, Hampe J, Yoshimura K, Noma T, Matsuzaki M, et al. Direct activation of mitochondrial apoptosis machinery by c-Jun N-terminal kinase in adult cardiac myocytes. J Biol Chem 2002;277:10244–50. [PubMed: 11786558]
44. Nishitoh H, Matsuzawa A, Tobiume K, Saegusa K, Takeda K, Inoue K, et al. ASK1 is essential for endoplasmic reticulum stress-induced neuronal cell death triggered by expanded polyglutamine repeats. Genes Dev 2002;16:1345–55. [PubMed: 12050113]
45. Urano F, Wang X, Bertolotti A, et al. Coupling of stress in the ER to activation of JNK protein kinases by transmembrane protein kinase IRE1. Science 2000;287:664–6. [PubMed: 10650002]
46. Nawrocki ST, Carew JS, Pino MS, et al. Bortezomib sensitizes pancreatic cancer cells to endoplasmic reticulum stress-mediated apoptosis. Cancer Res 2005;65:11658–66. [PubMed: 16357177]
47. Harding HP, Zhang Y, Bertolotti A, Zeng H, Ron D. Perk is essential for translational regulation and cell survival during the unfolded protein response. Mol Cell 2000;5:897–904. [PubMed: 10882126]
48. Lovat PE, Corazzari M, Armstrong JL, Martin S, Pagliarini V, Hill D, et al. Increasing melanoma cell death using inhibitors of protein disulfide isomerases to abrogate survival responses to endoplasmic reticulum stress. Cancer Res 2008;68:5363–9. [PubMed: 18593938]
49. Piva R, Ruggeri B, Williams M, Costa G, Tamagno I, Ferrero D, et al. CEP-18770: a novel, orally active proteasome inhibitor with a tumor-selective pharmacologic profile competitive with Bortezomib. Blood 2008;111:2765–75. [PubMed: 18057228]
50. Lee EF, Czabotar PE, Smith BJ, Deshayes K, Zobel K, Colman PM, et al. Crystal structure of ABT-737 complexed with Bcl-x_L: implications for selectivity of antagonists of the Bcl-2 family. Cell Death Differ 2007;14:1711–3. [PubMed: 17572662]

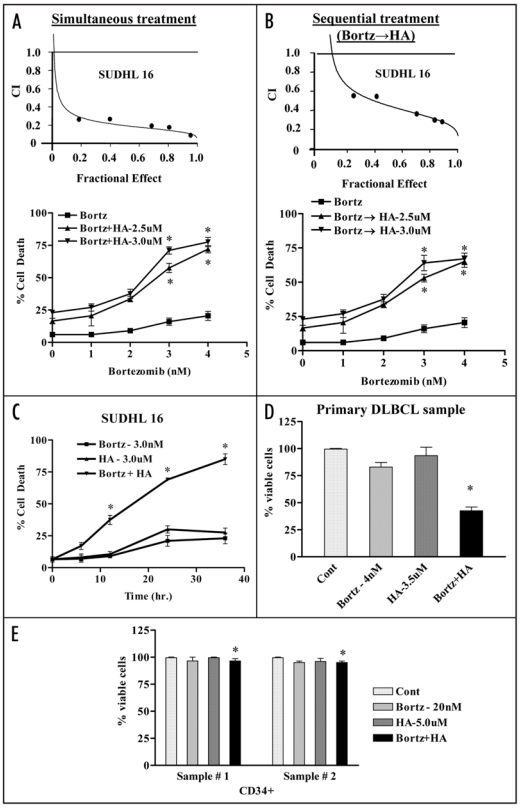

Figure 1.

Co-treatment of bortezomib and Bcl-2 antagonist leads to synergistic induction of cell death in DLBCL cells in a time dependent manner but not in normal hematopoietic cells. SUDHL16 cells were treated with indicated concentration of bortezomib ± HA14-1. (A) simultaneously or (B) sequentially (8 h bortezomib pretreatment followed by HA14-1) for a total of 36 h, after which cell death was monitored by flow cytometry with 7AAD staining. Insets (A and B): Fractional Effect (FA) values were determined by comparing results to those of untreated controls, and Median Dose Effect analysis was employed to characterize the nature of the interaction. Combination Index (C.I.) values less than 1.0 denote a synergistic interaction. Two additional studies yielded equivalent results. (C) SUDHL6 cells were treated with bortezomib ± HA14-1 at the indicated concentrations for various intervals, and cell death was determined by flow-cytometry with 7AAD staining (D) Primary human bone marrow DLBCL cells were isolated as described in Methods and suspended in medium containing 10% FCS at a cell density of 0.75×10^6/ml cells in the presence of 4 nM bortezomib ± 3.5 uM of HA14-1 for 14 h. At the end of drug exposure, apoptotic cells were monitored by Annexin/PI staining. Apoptotic cell death for controls was <25–20%. The percentage of non apoptotic cells were considered to represent the viable fraction, and values were normalized to controls. (E) $CD34^+$ cells obtained from the bone marrow of two patients undergoing routine diagnostic procedures for non-myeloid hematologic disorders were isolated by an immunomagnetic bead separation technique as described in Methods and exposed to bortezomib (20 nM) ± HA14-1 (5.0 μM) for 48 h. At the end of this period, the percentage of apoptotic cells was determined by Annexin V/PI staining and flow cytometry. The percentage of viable cells in each sample was normalized to controls. Values represent the means ± S.D. for triplicate determination. For (A–C), * = significantly greater than bortezomib alone; $p < 0.01$. For (D), * = not significantly different from values for untreated controls; $p > 0.05$.

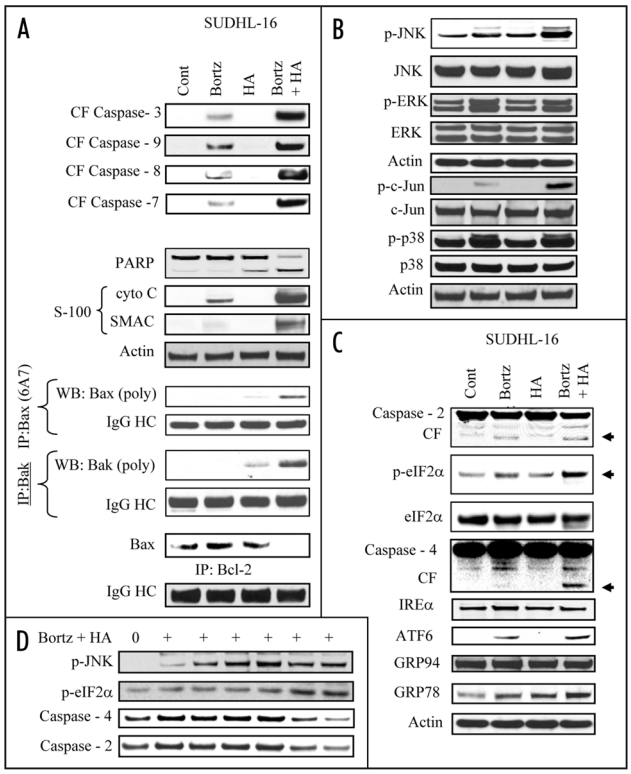

Figure 2.

Combined exposure to bortezomib and HA14-1 leads to a dramatic increase in caspase activation, mitochondrial damage, Bax and Bak translocation and conformational change, in association with JNK activation and ER stress induction in SUDHL16 cells. SUDHL16 cells were treated with 3 nM bortezomib ± 3.0 μM of HA14-1 for 14 h. (A) cytosolic (S-100) fractions were obtained as described in Materials and Methods, and expression of cytochrome *c*, AIF and Smac/DIABLO were monitored by western blot. Proteins from whole cell lysates were prepared and expression of the indicated proteins were determined by western blotting. Bax and Bak translocation and conformational change, as well as the association between Bax and Bcl-2 were monitored by immunoprecipitation followed by western blotting as described in Methods (B and C). At the end of the drug exposure (14 h) as (A) above, cells were lysed, sonicated, the proteins denatured, and subjected to western blot analysis using the indicated primary antibodies. (D) SUDHL 16 cells were treated with 3 nM bortezomib ± 3 μM HA14-1 for various intervals and changes in the expression of the indicated protein expression were monitored by western blotting. For these and all other studies, each lane was loaded with 30 μg of protein; blots were stripped and reprobed with antibodies directed against actin to ensure equivalent loading and transfer. Results are representative of three separate experiments.

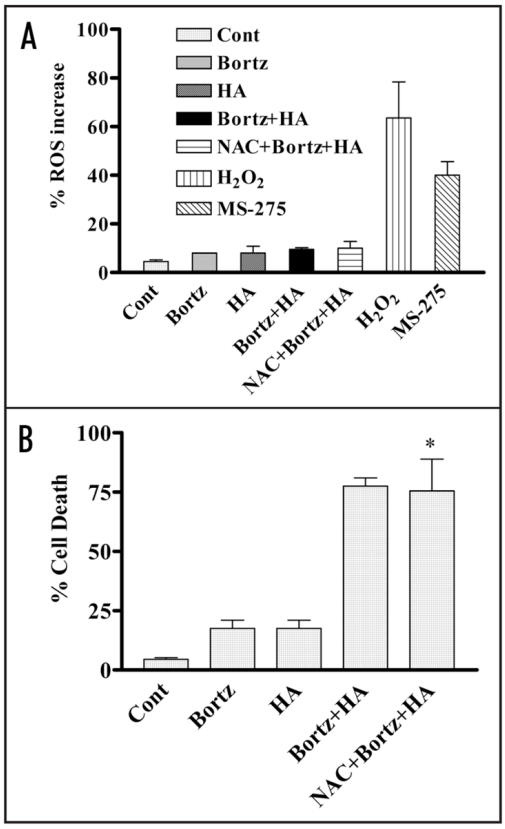

Figure 3.

Co-administration of bortezomib and HA14-1 fails to induce ROS generation and pretreatment with the antioxidant (NAC) fails to circumvent lethality in SUDHL4 cells. (A) SUDHL4 cells (preteated with or without 5 mM NAC for 3 h) were exposed to 5 nM bortezomib ± 4 μM HA14-1 for 4 h. Cells were also exposed to MS-275 (2 μM) or H_2O_2 (0.5 mM) for 30 min to serve as positive control for ROS generation. At the end of the exposure interval, ROS generation was monitored as described in Methods. (B) SUDHL4 cells (preteated with or without 5 mM NAC for 3 h) were exposed to 5 nM bortezomib ± 4 μM HA14-1 for 36 h. At the end of drug treatment, cell death was monitored by 7 AAD staining as described in methods. For (B), * = not significantly different from values for cells treated with bortezomib + HA14-1 in the absence of NAC; $p > 0.05$.

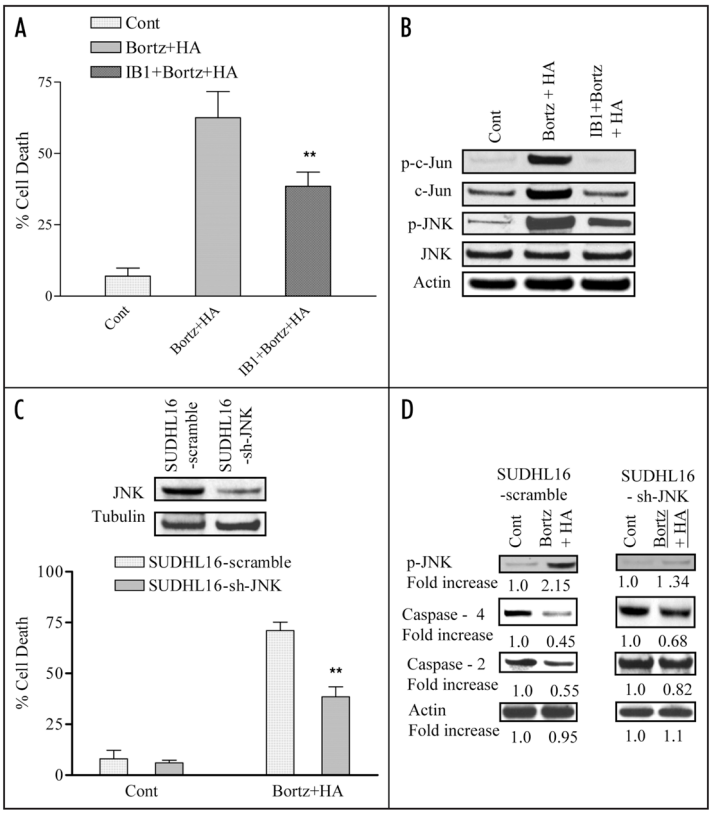

Figure 4.

Pharmacologic and genetic interruption of the JNK pathways significantly diminishes bortezomib/HA14-1 lethality in SUHDL16 cells. (A) SUDHL16 cells pretreated with the JNK inhibitor IB1 (ALX 159–600; 10 μM) for 2 hr were exposed to 3 nM bortezomib ± 3.0 μM HA14-1 for 36 hrs. At the end of drug exposure, apoptosis was monitored by 7 AAD staining and flow cytometry. ** = significantly less than values for cells treated in the absence of IB1; $p < 0.01$. (B) Cells were treated as above (A) for 14 hrs and western blot analysis was employed to monitor the effect of drugs on expression of the indicated proteins. Each lane was loaded with 30 μg of protein; blots were stripped and reprobed with antibodies directed against actin to ensure equivalent loading and transfer. The results of a representative study are shown; two additional studies yielded equivalent results. (C) SUDHL16 cells stably transfected with JNK shRNA or vectors encoding a scrambled sequence were exposed to 4.0 nM bortezomib + 4.0 μM HA14-1. After 36 hr of drug exposure, apoptotic cells were monitored by 7 AAD staining and flow cytometry. inset: relative expression of JNK protein in SUDHL16-scrambled sequence and shJNK clones (D) Following 14 hr of drug exposure as (C) above, western blot analysis was employed to monitor protein expression of phospho-JNK, caspase-4 and caspase 2. Blots were stripped and reprobed with anti-actin antibodies to ensure equal loading and transfer of protein For (A),** = significantly less than values for scrambled sequence clone; $p < 0.01$. For (C), ** = significantly less than values for empty-vector controls; $p < 0.05$.

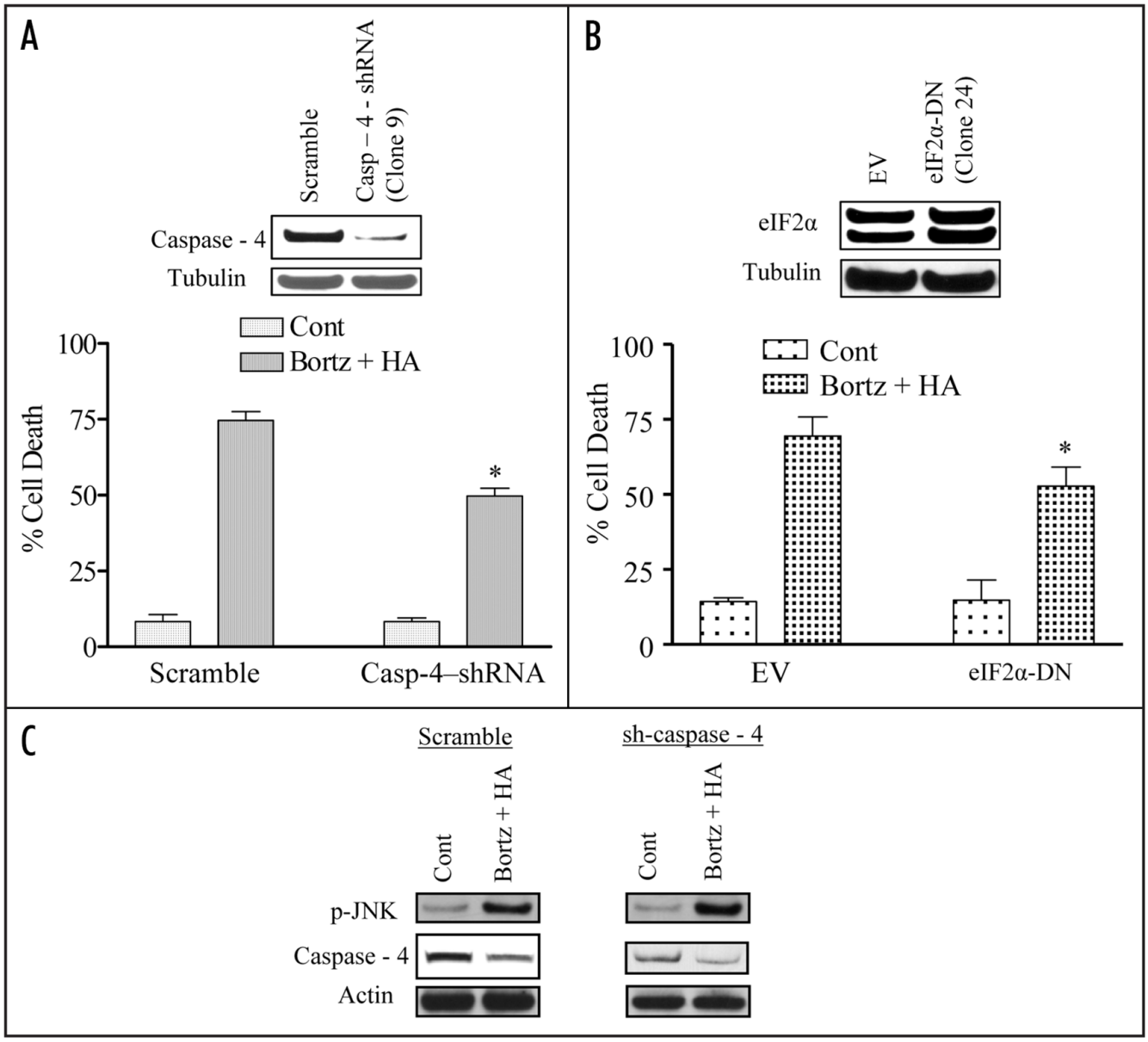

Figure 5.

Knockdown of caspase-4 expression or ecotopic expression of eIF2α-DN significantly diminishes bortezomib/HA14-induced lethality in SUDHL16 cells. (A) SUDHL16 cells stably transfected with caspase-4 shRNA or a scrambled sequence vector were exposed to 4.0 nM bortezomib + 4.0 μM HA14-1. Following 36 h of drug exposure, apoptotic cells were monitored by annexin V/PI staining and flow cytometry. Inset: relative expression of caspase 4 protein in scrambled sequence and shJNK clones. (B) SUDHL16 cells stably transfected with an eIF2α-DN or empty vector (pcDNA3.1) construct were incubated with 4 nM bortezomib + 4.0 μM HA14-1. After 36 h of drug exposure, apoptotic cells were monitored by annexin V/PI staining and flow cytometry. (C) Following 14 h of drug exposure to SUDHL16-casp4 shRNA cells as described in (A) above, western blot analysis was employed to monitor protein expression of caspase-4 and phospho-JNK. Blots were stripped and reprobed with anti-actin antibodies to ensure equal loading and transfer of

protein (30 μg each lane). For (A and B),* = significantly less than values for control cells; $p < 0.05$. Two additional studies yielded equivalent results.

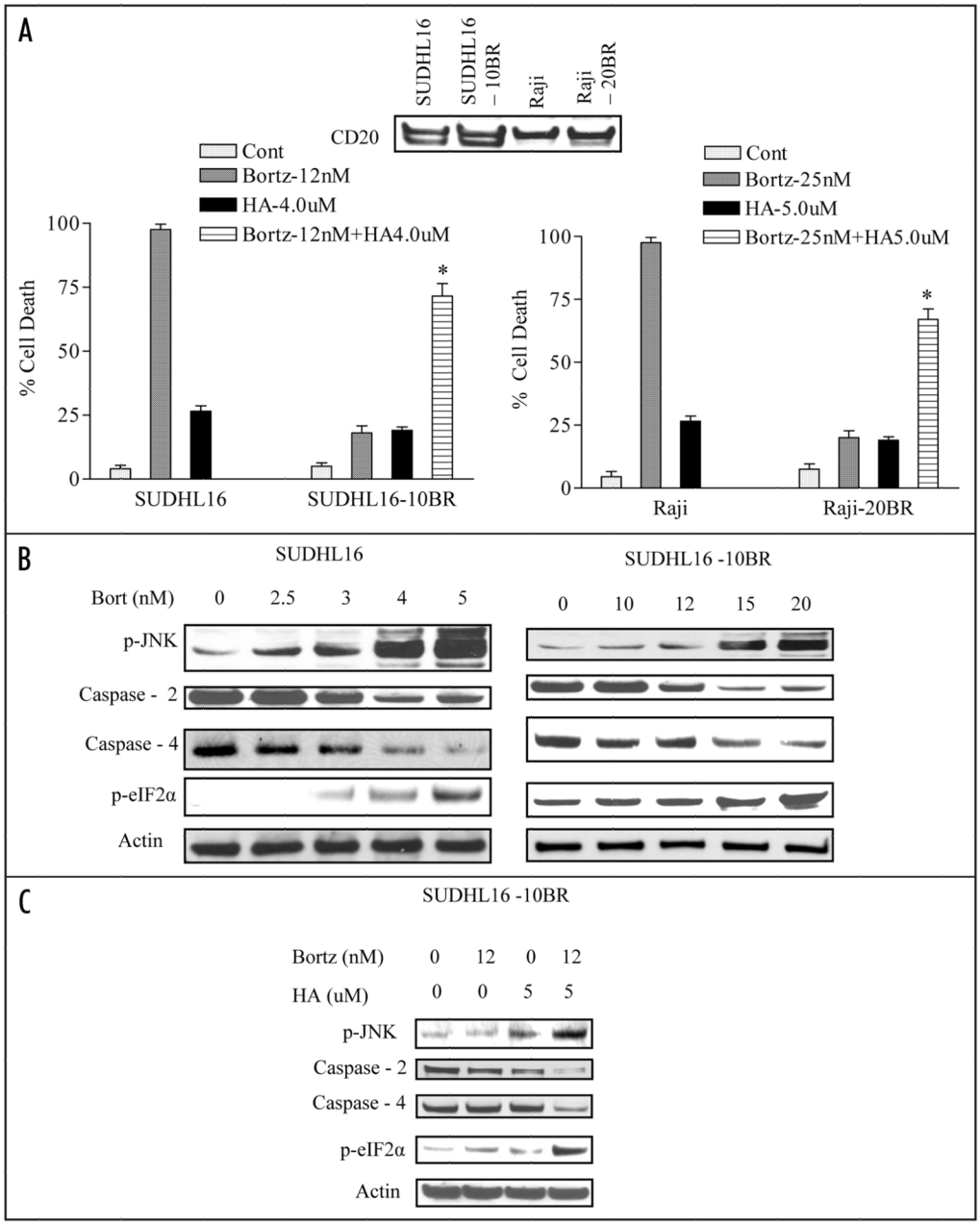

Figure 6.

HA14-1 increases the ability of bortezomib to induce JNK activation, evidence of ER stress, and lethality in bortezomib-resistant cells. (A) SUDHL16, SUDHL16-10BR, Raji and Raji-20BR cells were treated with the indicated concentrations of bortezomib ± HA14-1 for 36 and 48 h respectively after which cell death was assessed by flow cytometry using 7AAD staining. Inset: immuno-blotting depicting the expression of CD20 in parental and bortezomib-resistant cells. (B) SUDHL16, SUDHL16-10BR cells were treated with indicated concentration of bortezomib for 14 h. At the end of drug exposure, cells were lysed and equivalent amounts (30 μg) of protein subjected to immunoblotting with the indicated antibodies (C) SUDHL16-10BR cells were treated with the indicated concentration of bortezomib ± HA14-1 for 14 h. At the end of drug exposure, cells were lysed and equivalent amounts (20 μg) of protein were subjected to immunoblotting with

antibodies as indicated. In each case, blots were stripped and probed with antibodies directed against actin to ensure equivalent loading and transfer of proteins. For (A), * = significantly greater than values for bortezomib alone; $p < 0.01$.